

## Supporting Information

### Rechargeable Aqueous Phenazine-Prussian Blue Proton Battery with Long Cycle Life

Xiaoqing Zhang,<sup>‡a</sup> Xin Zhang,<sup>‡a</sup> Yao Miao,<sup>a</sup> Qinghong Huang,<sup>b,c</sup> Zhidong Chen,<sup>a</sup> Dengfeng Guo,<sup>a</sup> Juan Xu,\*<sup>a</sup> Yong-Miao Shen<sup>d</sup> and Jianyu Cao\*<sup>a</sup>

<sup>a</sup>*Jiangsu Key Laboratory of Advanced Catalytic Materials and Technology, School of Petrochemical Engineering, Changzhou University, Changzhou, 213164, China. E-mail: jycao@cczu.edu.cn (J. Cao); cjytion@cczu.edu.cn (J. Xu)*

<sup>b</sup>*College of Energy Science and Engineering, Nanjing Tech University, Nanjing 211816, China*

<sup>c</sup>*Jiangsu Key Laboratory of Materials Surface Science and Technology, Changzhou 213164, China.*

<sup>d</sup>*Key Laboratory of Excited-State Materials of Zhejiang Province, Department of Chemistry, Zhejiang Sci-Tech University, Hangzhou 310018, China.*

‡These authors contributed equally to this work.

\*Corresponding author, E-mail: jycao@cczu.edu.cn(J. Cao); cjytion@cczu.com (J. Xu)

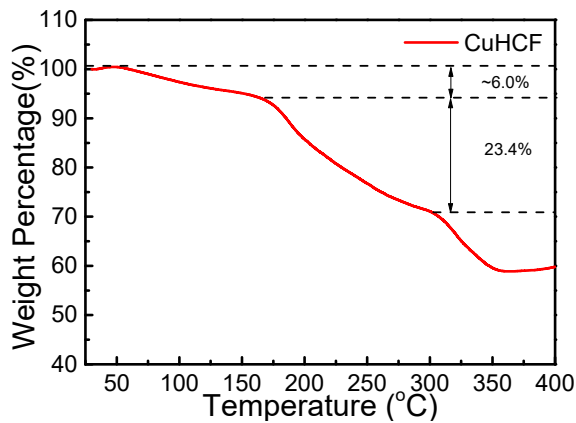


**Fig. S1** Thermogravimetric (TG) curve for as-prepared CuHCF measured in nitrogen atmosphere at a heating rate of  $10\text{ }^{\circ}\text{C min}^{-1}$ .

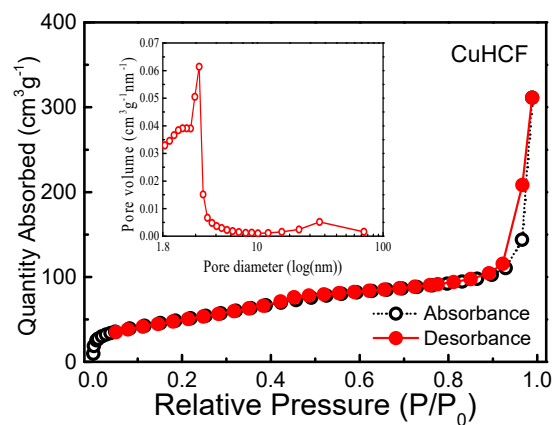


**Fig. S2** N<sub>2</sub> adsorption-desorption isotherm and BJH pore size distribution for CuHCF.

**Table S1** Textural properties of CuHCF.

Sample	S <sub>BET</sub> (m <sup>2</sup> g <sup>-1</sup> )	V <sub>pore</sub> (cm <sup>3</sup> g <sup>-1</sup> )	d <sub>BJH</sub> (nm)
CuHCF	185.0	0.47	3.7

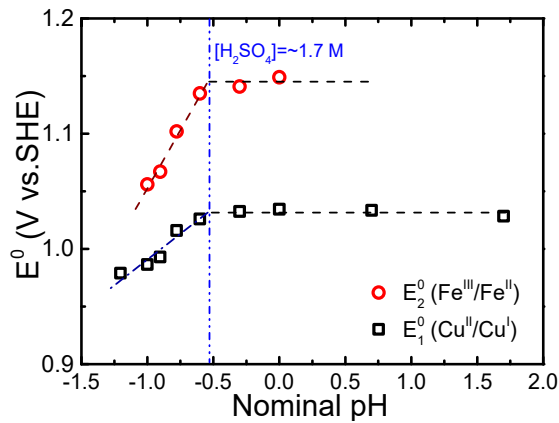


**Fig. S3** Pourbaix diagram ( $E^0$  vs. nominal pH) of CuHCF in sulfuric acid solutions of different concentrations (0.1~8 M).

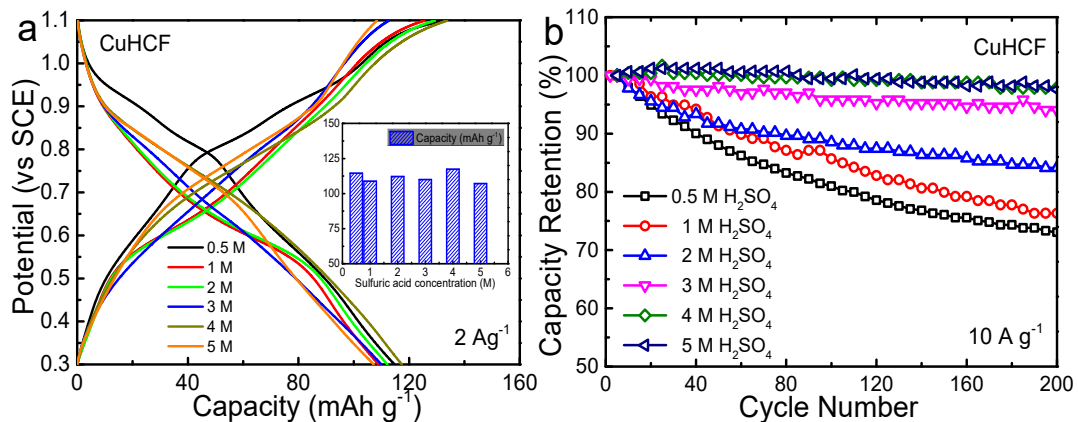


**Fig. S4** (a) Galvanostatic charge-discharge profiles of the CuHCF electrode at  $2 \text{ A g}^{-1}$  in sulfuric acid solutions of different concentrations. The inset of (a) is the plot of capacity versus sulfuric acid concentration. (b) Capacity retention of the CuHCF electrode at  $10 \text{ A g}^{-1}$  in sulfuric acid solutions of different concentrations.

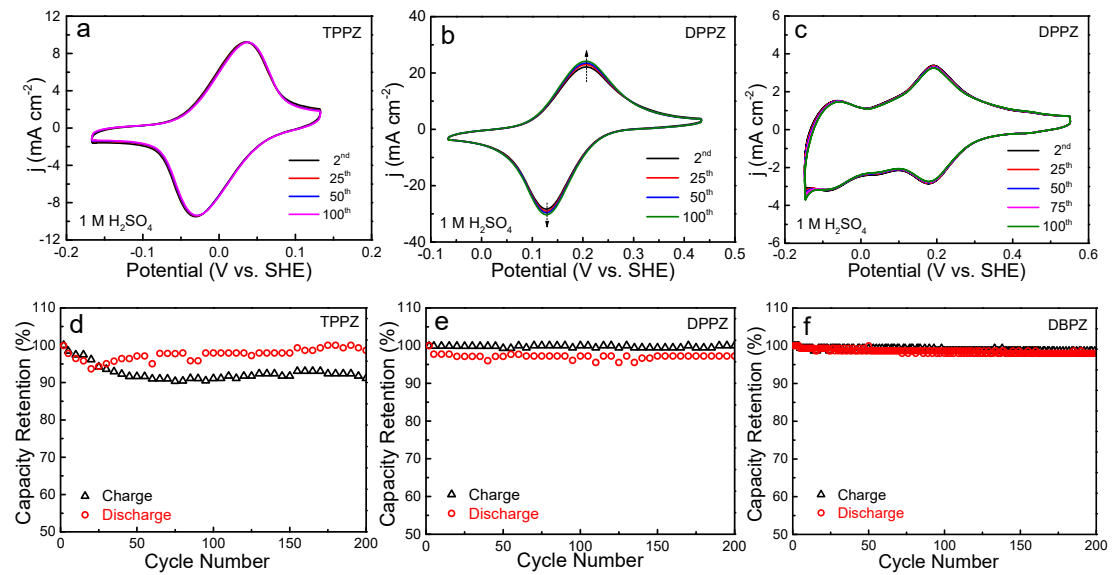


**Fig. S5** CVs of TPPZ (a), DPPZ (b) and DBPZ (c) electrodes in 1 M H<sub>2</sub>SO<sub>4</sub> solution at 100 mV s<sup>-1</sup> during the 2<sup>nd</sup>, 25<sup>th</sup>, 50<sup>th</sup> and 100<sup>th</sup> cycles. Capacity retentions of the TPPZ (d), DPPZ (e) and DBPZ (f) electrodes at 10 A g<sup>-1</sup> in 1 M H<sub>2</sub>SO<sub>4</sub> solution.

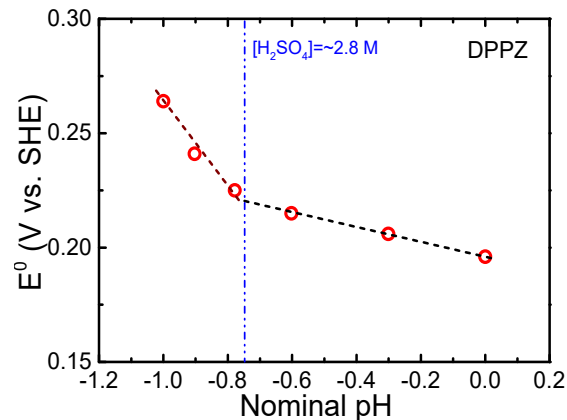


**Fig. S6** Pourbaix diagram (E° vs. nominal pH) of DPPZ in sulfuric acid solutions of different concentrations (0.5~5 M).

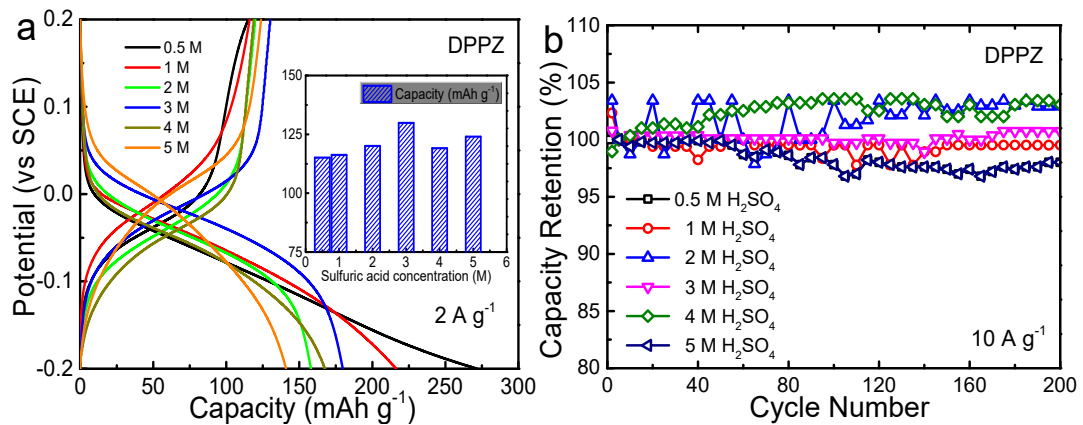


**Fig. S7** (a) Galvanostatic charge-discharge profiles of the DPPZ electrode at  $2 \text{ A g}^{-1}$  in sulfuric acid solutions of different concentrations. The inset of (a) is the plot of capacity versus sulfuric acid concentration. (b) Capacity retention of the DPPZ electrode at  $10 \text{ A g}^{-1}$  in sulfuric acid solutions of different concentrations.

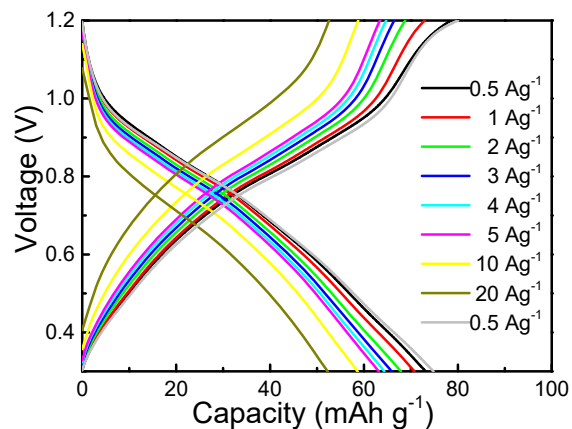


**Fig. S8** The GCD profiles of the DPPZ//CuHCF APB in a  $3 \text{ M H}_2\text{SO}_4$  aqueous electrolyte at several current densities between 0.3 and 1.2 V.

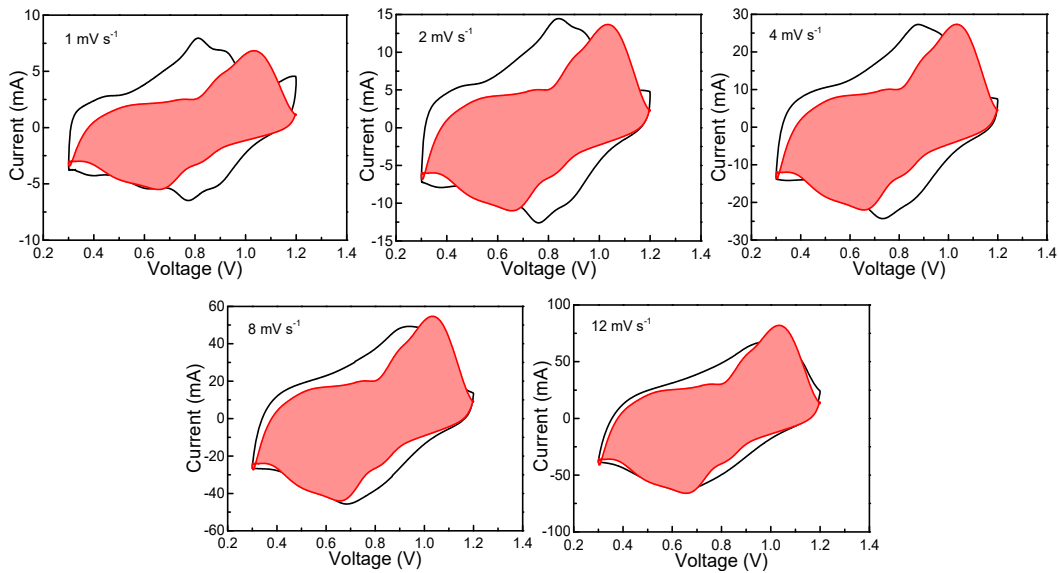


**Fig. S9** The CV profiles with the capacitive contribution of APBs at the scan rate of 1, 2, 4, 8 and 12  $\text{mV s}^{-1}$ , respectively.

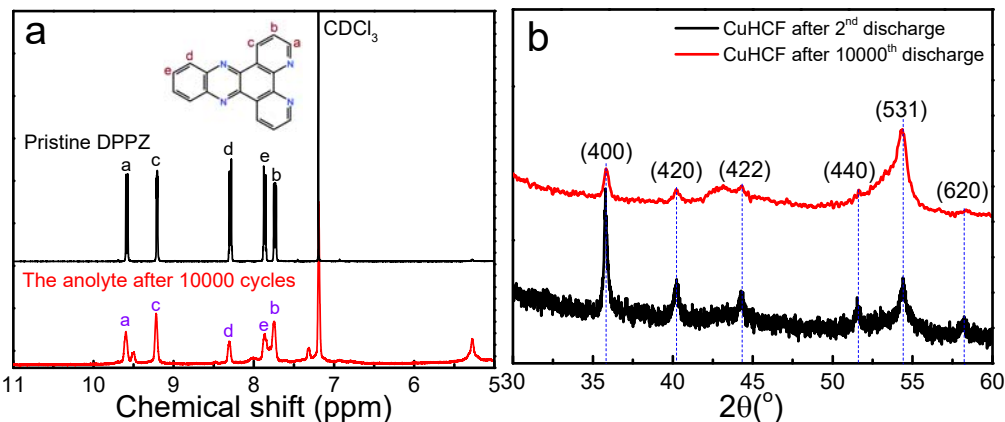


**Fig. S10** (a)  $^1\text{H}$  NMR spectrum of substances extracted from the anolyte after 10,000 cycles with chloroform ( $\text{CHCl}_3$ ). (b) XRD patterns for CuHCF cathodes after the 2<sup>nd</sup> and 10,000<sup>th</sup> cycles.

The five well-defined proton peaks attributed to DPPZ was observed in the anolyte after 10,000 cycles (Fig. S10a), indicating the dissolution of DPPZ or its reduced form during the charge-discharge process. The XRD diffraction peak position was basically identical for the CuHCF cathode before and after the long-term cycle, indicating that the crystalline structure of CuHCF was still maintained.

**Table S2** A performance summary of aqueous proton batteries (APBs). OCV, open circuit voltage. Capacity and energy density are calculated based on the total weight of both active electrode materials. NA, not applicable. AQDS, anthraquinone-2,7-disulfonate. CRP, conducting redox polymer. DPPZ, dipyridophenazine. InHCF, indium hexacyanoferrate. AQ, anthraquinone. TCHQ, tetrachlorohydroquinone. CuHCF, copper hexacyanoferrate. pDTP-AQ, poly(dithieno[3,2-b:2',3'-d] pyrrole) N-twisted anthraquinone pendants. pDTP-NQ2H, poly(dithieno[3,2-b:2',3'-d] pyrrole) N-twisted naphthohydroquinone pendants. PNAQ, poly(aminoanthraquinone). PUQ, AQ-based polyurethane. PTC, a catechol-based poly(3,4-ethylenedioxythiophene) (PEDOT). PO, poly(2,9-dihydroquinoxalino[2,3-b] phenazine). PR, fully reduced PO. NiHCF, nickel hexacyanoferrate.

Battery type	OCV (V)	Capacity (mAhg <sup>-1</sup> )	Coulomb efficiency	Energy density (Wh kg <sup>-1</sup> )	Energy efficiency	Capacity retention
Alizarin//Alizarin <sup>[S1]</sup>	1.04	81.5 (at 10 C)	95% (at 10 C)	~81 (at ~1.6 A g <sup>-1</sup> )	>80% (at 10 C)	47% at 10 C (~1.6 A g <sup>-1</sup> ) for 100 cycles (99.25% per cycle)
Alizarin//2,3-CH <sub>3</sub> -quinizarin <sup>[S1]</sup>	1.16	~82 (at 10 C)	~88% (at 10 C)	NA	NA	55% at 10 C for 500 cycles (99.88% per cycle)
AQDS//tiron <sup>[S2]</sup>	<0.7	54 (at 1 C)	99.4% (at 5 C)	28.5 (at 1 C)	78% (at 5 C)	70% at 5 C (~0.27 A g <sup>-1</sup> ) for 600 cycles (99.94% per cycle)
pEP(NQ)E//pEP(QH <sub>2</sub> )E <sup>[S3]</sup>	0.4	~45 (at 3 C)	NA	~18 (at 3 C)	NA	85% at 3C (0.18 A g <sup>-1</sup> ) for 500 cycles (99.968% per cycle)
DPPZ//InHCF <sup>[S4]</sup>	0.82	37 (at 1 A g <sup>-1</sup> )	99.7% (at 6 Ag <sup>-1</sup> )	~28 (at 1 A g <sup>-1</sup> )	69.5% (at 6 Ag <sup>-1</sup> )	76.1% at 6 A g <sup>-1</sup> (~52 C) for 3000 cycles (99.991% per cycle)
AQ//TCHQ <sup>[S5]</sup>	0.61	~53 (at 0.45 A g <sup>-1</sup> )	NA	30.6 (at 45 mA g <sup>-1</sup> )	NA	70.8% at 0.225 A g <sup>-1</sup> (5 C) for 500 cycles (99.931% per cycle)
CuHCF half-cell <sup>[S6]</sup>	NA	95* (at 1 C)	NA	NA	NA	60% at 500 C for 730,000 cycles (99.99993% per cycle)

MoO <sub>3</sub> //CuHCF <sup>[S7]</sup>	~1.0	46 (at 2 A g <sup>-1</sup> )	~98% (at 2 A g <sup>-1</sup> )	40 (at 2 A g <sup>-1</sup> )	NA	85% at 2 A g <sup>-1</sup> for 1000 cycles (99.984% per cycle)
pDTP-AQ//pDTP-NQ2H <sup>[S8]</sup>	0.34	78 (at 0.5 A g <sup>-1</sup> )	~95% (at 1 A g <sup>-1</sup> )	23.4 (at 0.5 A g <sup>-1</sup> )	NA	56% at 1 A g <sup>-1</sup> for 2000 cycles (99.971% per cycle)
Pt/H <sub>2</sub> /H <sup>+</sup> //CuHCF <sup>[S9]</sup>	~0.84	52 (at 10 C)	99.8% (at 960 C)	43.3 (at 10 C)	70% (at 1 C)	62% at 960 C for 350,000 cycles (99.99986% per cycle)
PNAQ//PNAQ <sup>[S10]</sup>	~0.65	42.7 (at 0.6 A g <sup>-1</sup> )	~99% (at 6 A g <sup>-1</sup> )	~25.2 (at 0.6 A g <sup>-1</sup> )	NA	70% at 50 C (6 A g <sup>-1</sup> ) for 500 cycles (99.929% per cycle)
PUQ//PTC <sup>[S11]</sup>	0.72	~39 (at 0.5 A g <sup>-1</sup> )	~98% (at 2 A g <sup>-1</sup> )	~24 (at 0.5 A g <sup>-1</sup> )	NA	80% at 2 A g <sup>-1</sup> for 1000 cycles (99.978% per cycle)
PR//PO <sup>[S12]</sup>	0.65	147 (at 0.1 A g <sup>-1</sup> )	~100% (at 1 A g <sup>-1</sup> )	88.2 (at 0.1 A g <sup>-1</sup> )	~82% (at 0.1 A g <sup>-1</sup> )	94% at 1 A g <sup>-1</sup> for 500 cycles (99.988% per cycle)
MoO <sub>3</sub> //NiHCF <sup>[S13]</sup>	0.56& 0.97	62.6 (at 0.5 A g <sup>-1</sup> )	99.5% (at 1 A g <sup>-1</sup> )	~41 (at 0.5 A g <sup>-1</sup> )	NA	76.1% at 1 A g <sup>-1</sup> for 400 cycles (99.932% per cycle)
<b>DPPZ//CuHCF (this work)</b>	<b>~0.84</b>	<b>74.3 (at 0.5 A g<sup>-1</sup>)</b>	<b>~100% (at 10 A g<sup>-1</sup>)</b>	<b>52.0 (at 0.5 A g<sup>-1</sup>)</b>	<b>87.1% (at 10 A g<sup>-1</sup>)</b>	<b>65.2% at 10 A g<sup>-1</sup> for 10000 cycles (99.9957% per cycle)</b>

\* Based the cathode materials.

## References

- [S1] L. Tong, Y. Jing, R. G. Gordon, M. J. Aziz, ACS Appl. Energy Mater. 2019, 2, 4016-4021.
- [S2] Y. Xu, Y. Zheng, C. Wang, Q. Chen, ACS Appl. Mater. Interfaces 2019, 11, 23222-23228.
- [S3] C. Strietzel, M. Sterby, H. Huang, M. Strømme, R. Emanuelsson, M. Sjödin, Angew. Chem. Int. Ed. 2020, 59, 9631-9638.
- [S4] J. Qiao, M. Qin, Y.-M. Shen, J. Cao, Z. Chen, J. Xu, Chem. Commun., 2021, 57, 4307-4310.
- [S5] K. Nueangnoraj, T. Tomai, H. Nishihara, T. Kyotani, I. Honma, Carbon 2016, 107, 831-836.
- [S6] X. Wu, J. J. Hong, W. Shin, L. Ma, T. Liu, X. Bi, Y. Yuan, Y. Qi, T. W. Surta, W. Huang, J. Neuefeind, T. Wu, P. A. Greaney, J. Lu, X. Ji, Nat. Energy, 2019, 4, 123-130.
- [S7] H. Jiang, W. Shin, L. Ma, J. J. Hong, Z. Wei, Y. Liu, S. Zhang, X. Wu, Y. Xu, Q. Guo, M. A. Subramanian, W. F. Stickle, T. Wu, J. Lu, X. Ji, Adv. Energy Mater. 2020, 10, 2000968.
- [S8] X. Wang, J. Zhou, W. Tang, Energy Stor. Mater. 2021, 36, 1-9.
- [S9] Z. Zhu, W. Wang, Y. Yin, Y. Meng, Z. Liu, T. Jiang, Q. Peng, J. Sun, W. Chen, J. Am. Chem. Soc. 2021, 143, 20302-20308.
- [S10] T. Sun, H. Du, S. Zheng, J. Shi, X. Yuan, L. Li, Z. Tao, Small Methods 2021, 5, 2100367.
- [S11] M. Zhu, L. Zhao, Q. Ran, Y. Zhang, R. Peng, G. Lu, X. Jia, D. Chao, C. Wang,

Adv. Sci. 2022, 9, 2103896.

[S12] Z. Tie, S. Deng, H. Cao, M. Yao, Z. Niu, J. Chen, Angew. Chem. Int. Ed. 2022, 134, e202115180.

[S13] B. Yang, T. Qin, Y. Du, Y. Zhang, J. Wang, T. Chen, M. Ge, D. Bin, C. Ge, H. Lu, Chem. Commun., 2022, 58, 1550-1553.